

SCIENTIFIC REPORTS



OPEN

Microbial Competition of *Rhodotorula mucilaginosa* UANL-001L and *E. coli* increase biosynthesis of Non-Toxic Exopolysaccharide with Applications as a Wide-Spectrum Antimicrobial

Augusto Vazquez-Rodriguez^{1,2}, Ximena G Vasto-Anzaldo³, Daniel Barboza Perez^{1,2}, Eduardo Vázquez-Garza^{4,5}, Héctor Chapoy-Villanueva^{4,5}, Gerardo García-Rivas^{4,5}, Javier A. Garza-Cervantes¹, Jéssica J. Gómez-Lugo^{1,2}, Alma Elizabeth Gomez-Loredo^{1,2}, Maria Teresa Garza Gonzalez^{1,2}, Xristo Zarate^{1,2} & Jose Ruben Morones-Ramirez^{1,2}

Bacterial species are able to colonize and establish communities in biotic and abiotic surfaces. Moreover, within the past five decades, incidence of bacterial strains resistant to currently used antibiotics has increased dramatically. This has led to diverse health issues and economical losses for different industries. Therefore, there is a latent need to develop new and more efficient antimicrobials. This work reports an increased production of an exopolysaccharide in a native yeast strain isolated from the Mexican Northeast, *Rhodotorula mucilaginosa* UANL-001L, when co-cultured with *E. coli*. The exopolysaccharide produced is chemically and physically characterized and its applications as an antimicrobial and antibiofilm are explored. The exopolysaccharide is capable of inhibiting planktonic growth and biofilm formation in *Escherichia coli*, *Pseudomonas aeruginosa* and *Staphylococcus aureus*. Additionally, the exopolysaccharide studied here does not exhibit cytotoxic effects when assessed both, *in vitro* against an H9c2 mammalian cell line, and *in vivo* in a murine toxicity model. Taken together, the properties of this exopolysaccharide indicate that it has potential applications to inhibit bacterial colonization in medical and industrial settlings.

Within the last five decades there has been an increased frequency in the emergence of bacterial strains resistant to commercially available antibiotics¹⁻⁴. Therefore, there is an urgent need to seek, develop and design new antimicrobials to treat infections and to combat bacterial strains in industrial settings⁵. Bacteria have the ability to colonize biotic and abiotic environments through the formation of biofilms⁶. It has been estimated that 80% of bacterial infections in humans are caused by bacterial biofilms, and 50% of the nosocomial infections are

¹Universidad Autónoma de Nuevo León, Facultad de Ciencias Químicas, Pedro de Alba, S/N, San Nicolas de los Garza, Nuevo León, Mexico. ²Centro de Investigación en Biotecnología y Nanotoxicología, Facultad de Ciencias Químicas, Universidad Autónoma de Nuevo León. Parque de Investigación e Innovación Tecnológica, Km. 10 autopista al Aeropuerto Internacional Mariano Escobedo, Apodaca, Nuevo León, 66629, Mexico. ³Universidad Autónoma de Nuevo León, Facultad de Ciencias Biológicas, Pedro de Alba, S/N, San Nicolas de los Garza, Nuevo León, Mexico. ⁴Cátedra de Cardiología y Medicina Vascul. Escuela de Medicina. Tecnológico de Monterrey, Monterrey, Nuevo León, Mexico. ⁵Centro de Investigación Biomédica. Hospital Zambrano-Hellion. Tecnológico de Monterrey, San Pedro Garza-García, Nuevo León, Mexico. Correspondence and requests for materials should be addressed to J.R.M.-R. (email: jose.moronesr@uanl.edu.mx)

Yeast Mold Media (YM)		Yeast Mold Mineral Media (YMM)		Yeast Mold Mineral Media with added Zn (YMMZ)	
Ingredient	Conc. (g/L)	Ingredient	Conc. (g/L)	Ingredient	Conc.(g/L)
Yeast Extract	5	Yeast Extract	2	Yeast Extract	2
Dextrose	20	Dextrose	20	Dextrose	20
Malt Extract	3	KH ₂ PO ₄	1	KH ₂ PO ₄	1
Peptone	5	NaCl	0.1	NaCl	0.1
		MgSO ₄ ·7H ₂ O	0.5	MgSO ₄ ·7H ₂ O	0.5
		CaCl ₂	0.1	CaCl ₂	0.1
		NH ₄ Cl	2	NH ₄ Cl	2
				ZnSO ₄ ·7H ₂ O	0.05

Table 1. Composition of the different tested to grow *R. mucilaginosa* UANL-001L.

acquired due to biofilm-infected medical devices⁷. Moreover, the presence of biofilms is one of the leading causes of recurring infections and emergence of resistant strains, which has led to both health issues and large economical losses⁸. It is therefore imperative to develop new antimicrobials with the ability to control both planktonically grown bacteria and those found within biofilms^{9,10}.

In nature, microorganisms establish complex communities that communicate and interact through diverse beneficial and antagonistic interactions. Antagonistic interactions in many cases involve the production of a myriad of compounds that induce microbial inhibition and bacterial cell damage¹¹. Fungi are of particular interest since these microorganisms are usually capable of producing a broad range of metabolites that allow them to modify the physicochemical properties of their surroundings and control populations of their bacterial neighbors¹². Particularly, many yeasts are able to synthesize and secrete exopolysaccharides (EPS), biopolymers comprised of different monosugar units that present different conformations and structures^{13–15}. It has been observed that the biological function of EPS is closely related to their configuration and one of the biological functions found in some exopolysaccharides is their ability to inhibit bacterial growth^{16–19}.

EPS are mainly produced when microbial cells are under stressful conditions, since their overproduction is a defense mechanism against different microorganisms and toxins²⁰. Particularly, EPS act as a matrix for biofilm formation, offering a protective barrier against physical and chemical stressors. Additionally, in rare occasions, EPS can act as molecules that inhibit the biofilm formation process of competing microorganisms^{21,22}.

Recently, diverse authors have identified and isolated a variety of exopolysaccharides from different microorganisms, such as microalgae, bacteria, plants and fungi. Some of these EPS exhibit antimicrobial and antibiofilm activity when tested against distinct bacterial strains^{23,24}. It is therefore of interest to study the properties of novel EPS produced by different microbial species, since, in some cases, they are capable of controlling microbial proliferation and biofilm formation.

Our research group recently isolated a metal-resistant *Rhodotorula mucilaginosa* UANL-001L yeast strain from an industrial water effluent contaminated with different heavy metals²⁵. The strain was found to be capable of producing higher EPS yields under metal-stress conditions²⁵. In this work, we find that *Rhodotorula mucilaginosa* UANL-001L increases EPS biosynthesis, when co-cultured with *E. coli*. We therefore suggested that this increased production could be linked to a defense mechanism in *Rhodotorula mucilaginosa* UANL-001L. This led us to explore antimicrobial and antibiofilm properties of the produced EPS. We report here that the EPS produced by the autochthonous strain exhibit interesting antimicrobial and antibiofilm properties against different Gram-negative and Gram-positive organisms. The EPS produced are chemically and physically characterized and, to dimension their possible applications in industry and as therapeutic agents, their cytotoxic effects are assessed, *in vitro* using mammalian cell cultures and *in vivo* through a murine toxicity model.

Material and Methods

Growth Conditions of Different Strains Used. The yeast strain used in this work was *Rhodotorula mucilaginosa* UANL-001L. The strain was isolated from the water streams of the Pesqueria River, located in the state of Nuevo Leon in the Northeast of Mexico. The inoculum was conserved at -80°C in YM broth (Difco, BD) supplemented with 20% (V/V) glycerol.

Three exploratory media cultures were tested: Yeast Mold (YM), Yeast Mold Mineral (YMM) and YMMZ (Yeast Mold Mineral with added Zn). The specific compositions of each of the media are displayed in Table 1.

All experimental cultures of *R. mucilaginosa* UANL-001L were grown in 500 mL Erlenmeyer flasks, containing 200 mL of media. Afterwards, all additional experiments were performed, unless otherwise stated, in 500 mL Erlenmeyer flasks with 200 mL of YMMZ. All cultures were inoculated with a 2 mL aliquot obtained from an overnight yeast culture at an OD_{600nm} of 1. Unless otherwise indicated, all cultures of *R. mucilaginosa* UANL-001L were grown at 28 °C and 200 rpm for 96 h.

In this study different bacterial strains were used: *E. coli* ATCC 11229, *Staphylococcus aureus* ATCC 6538 and *Pseudomonas aeruginosa* ATCC 27853. These were conserved in LB broth media (Difco, BD) supplemented with 20%(v/v) glycerol. Unless otherwise indicated all of the experimental bacterial cultures were grown in LB broth at 37 °C and 150 rpm for 12 hours.

Growth Conditions of *Rhodotorula mucilaginosa* UANL-001L and *E. coli* Co-cultures. For the co-culture experiments, *E. coli* ATCC 11229 was grown in the presence of *R. mucilaginosa* UANL-001L in 500 mL

Erlenmeyer flasks, containing 200 mL of YM (Yeast Mold) media with different concentrations of added glucose (5, 10 and 15 g/L). The flasks were inoculated with an overnight culture of each of the strains (*E. coli* and *R. mucilaginosa*) and they were grown for 72 h at 28 °C and 140 rpm. The inoculum was set to include 1×10^6 CFU/mL of *R. mucilaginosa* and a variable inoculum of *E. coli* at three different initial concentrations (1×10^6 , 3×10^6 and 5×10^6 CFU/mL). After 72 h the biomass from the co-culture was separated from supernatant and the EPS in the supernatant was collected. The extraction and purification of the EPS is thoroughly described in the next section.

Separation and Purification of EPS. In order to produce exopolysaccharide, the production media broth (200 mL) was inoculated with 1% of an overnight culture ($OD_{600} = 1$) of the *Rhodotorula mucilaginosa* strain (UANL-001L) and grown at 28 °C and 200 rpm for 96 h. Once the yeast culture reached exponential phase, the biomass was separated from the supernatant by centrifuging the culture at 10,000 rpm for 20 min. Next, the supernatant (containing the EPS) was filtrated through a 0.45 μ m pore diameter membrane filter (Milipore). Then, 96% ethanol was added to the filtered supernatant in a 3:1 volume ratio to precipitate the EPS contained in the filtered supernatant sample. The ethanol/supernatant mixture was maintained at 4 °C for 12 hours. Subsequently, the mixture was centrifuged at 10,000 rpm for 20 minutes and the pellets (EPS) were separated from the liquid phase. The precipitated EPS were washed twice with 70% ethanol and, at each step the EPS were centrifuged at 10,000 rpm for 10 min. The recovered pellet was dissolved in deionized water and dialyzed using Spectra/Por molecular porous tubular dialysis membranes for 48 h. The final pellet was then freeze-dried overnight in a lyophilizer (Labconco Freezone-6 model). Finally, the EPS production yield was quantified gravimetrically. All experiments were run in triplicates.

Cell growth and EPS Kinetic Production. To study the relationship between cell growth and EPS production, *Rhodotorula mucilaginosa* UANL-001L cultures were adjusted to an initial cell density of 0.02 (OD_{600nm}) and grown at 28 °C and 250 rpm for 100 hours.

To measure cell growth, aliquots were taken at intervals of 12 hours to monitor OD_{600nm} and CFUs/mL using a plating method. To determine EPS production yield, samples were taken every 24 hours. EPS production yield was determined by precipitation and purification as previously described.

Scanning Electron Microscopy Analysis. Scanning Electron Microscopy was performed to study the surface morphology and porosity of the exopolysaccharide produced by *Rhodotorula mucilaginosa* UANL-001L. Micrographs were taken using a Nova NanoSEM 200 FEI scanning electron microscope with field emission.

FT-IR analysis. In order to identify functional groups in the exopolysaccharide produced by *Rhodotorula mucilaginosa* UANL-001L, an FT-IR spectrum of the EPS was performed using a Tensor 27 spectrometer (Bruker, Germany) in the region of 400–4000 cm^{-1} .

Chemical Characterization of EPS. Total amount of carbohydrates present in the EPS samples was determined using the Acid-Phenol Dubois Method²⁶. A carbohydrate calibration curve was constructed using glucose as the reference carbohydrate. The solution containing EPS was prepared by dissolving 10 mg of dried EPS in 10 mL of distilled water. A 1 mL aliquot was diluted with 1 mL of 80% (w/v) phenol in water and 5 mL of concentrated H_2SO_4 . The solution was then heated at 100 °C for 7 minutes. The sample was left at room temperature for 5 hours in order to cool and an aliquot was diluted 1:100 in concentrated H_2SO_4 to measure its absorbance at 490 nm using a Varian Cary 50 UV-Vis Spectrophotometer. All experiments were done in triplicates.

Detection of carbonyl groups in the EPS was performed by running a test with 2,4-Dinitrophenylhydrazine (DNPH, Brady's reagent)²⁷. 10 mg of dried EPS were dissolved in 10 mL of deionized water. Then, two drops of this sample, 2 mL of 95% ethanol and 3 mL of Brady's agent were added to a glass tube and all components were well mixed through vigorous agitation. The presence of a carbonyl group was determined by visually checking if a precipitate was formed in the reaction (positive test)²⁷.

Moreover, a qualitative elemental analysis was performed to detect chemical groups containing nitrogen in the EPS samples. 10 mg of the dried EPS were dissolved in 10 mL of deionized water. Two drops of a $Fe(NH_4)_2(SO_4)_2$ saturated solution, and 2 drops of 30% KF solution were added to a 1 mL glass tube and mixed well. The solution was alkalinized to a pH 9 using concentrated NaOH, and it was then slightly heated in a water bath at 60 °C for 10 seconds to finally be filtered using filter paper under vacuum. Two drops of an $FeCl_3$ saturated solution and enough H_2SO_4 was added to dissolve the $Fe(OH)_3$ and the solution was acidified. Finally the sample was boiled for 30 seconds and then added aliquots of 10% H_2SO_4 until a greenish-blue color appeared, indicating the presence of nitrogen²⁸.

Finally, elemental analysis to quantify carbon, nitrogen, hydrogen, and sulfur contents was performed using a Perkin Elmer 2400 Series II CHNS/O Elemental Analyzer. The reported elemental analysis is an average of the results from three EPS samples. The respective standard deviation is also reported.

Size Exclusion Chromatography. Size exclusion chromatography of EPS was performed using an Äkta Prime Plus FPLC system (GE Healthcare) with a Superdex 200 Increase 10/300 GL column (GE Healthcare). The column was equilibrated with 50 mM TRIS, 100 mM KCl, pH 7.5 buffer pre-filtered through a 0.22 μ m filter (Millipore) and a flow rate of 0.3 mL/min. Molecular size calibration was carried out using the gel filtration markers kit (Sigma Aldrich) including: cytochrome C (12.4 kDa), carbonic anhydrase from bovine erythrocytes (29 kDa), albumin bovine serum (66 kDa), alcohol dehydrogenase from yeast (150 kDa), amylase from sweet potato (200 kDa) and blue dextran (>2,00 kDa) under the same conditions. The purified EPS were dissolved in the same buffer and were run after calibration with the standards under the same conditions.

Monosaccharide composition analysis. *HPAEC-PAD.* 1 nmole each in 100 μ L was injected on a Dionex ICS-3000, HPAEC-PAD instrument. A CarboPac PA-1 column (4 \times 250 mm) was used for profiling of the monosaccharides using a NaOH/NaOAc gradient solvent mixture. Acidic sugars generally elute after 30 min. The EPS samples were hydrolyzed using 2 N TFA at 100 °C for 4 h, followed by removal of excess acid using dry nitrogen flush and then dissolved in water and a known amount was injected on HPAEC-PAD.

GC-MS analysis. The presence of each of the monosugars was confirmed by matching with the retention time of known monosaccharide standards and the GCMS spectrum. The EPS samples were methanolized using 1 M Methanolic-HCl at 80 °C for 16 h, followed by re-N-acetylation and TMS derivative of monosaccharides. Finally, the derivative monosaccharide was dissolved in hexane and injected on the GCMS, equipped with a Restek 5-ms capillary column. Helium was used as the carrier gas. Myo-inositol was used as an internal standard, only the detected monosaccharides are labeled.

Antibiofilm Activity of EPS. The antibiofilm assays were performed by first resuspending the lyophilized EPS in bidistilled water to produce a 400 mg/mL stock solution. The EPS stock solution was stored at 4 °C.

Antibiofilm activity of the EPS was analyzed by an adapted microtiter biofilm formation assay. Aliquots of each of the different bacteria cultures tested in this work were transferred into the 96-well microtiter plate obtaining a final dilution of 1:200. Afterwards, different concentrations of EPS were added to each well as follows: 2500 ppm, 2000 ppm, 1000 ppm, 500 ppm, 250 ppm, 125 ppm and 75 ppm. A control culture was grown in parallel without having added EPS. All biofilm cultures were incubated at 37 °C for 36 hours under static conditions.

Biofilm inhibition was measured using the crystal violet staining method²⁹. In order to discard planktonic cells from biofilm cultures, after the incubation period the supernatant was removed and each of the microtiter plates were washed 3 times with bidistilled water. The plates were then dried with hot air and the biofilm that remained in each well of the titer plates was stained with 250 μ L of 1% crystal violet dye for 10 minutes. After 10 minutes, the dye was washed away with bidistilled water. Biofilms were then de-stained by adding 250 μ L of an ethanol 96% solution. The ethanol/crystal violet dye solution at each of the wells is finally transferred to another microliter plate where the optical density is measured at 590 nm using a Varioskan (Thermo Scientific, Burlington, ON, Canada) spectrophotometer. The values are given as the mean of 6 biological replicates and their respective standard deviations are reported.

Bacterial Growth Inhibition with EPS. For the antimicrobial assays, the lyophilized EPS were resuspended in bidistilled water to produce a 400 mg/mL stock solution that was stored at 4 °C. The effect of EPS on bacterial growth and its antibacterial activity was assayed by the microdilution method. Suspensions of each of the different bacteria cultures tested were inoculated into a 96-well microtiter plate (10⁷ cells/well) and incubated in the presence of a range of different EPS concentrations as follows: 2500 ppm, 2000 ppm, 1000 ppm, 500 ppm, 250 ppm, 125 ppm and 75 ppm. As a control, a culture was grown in parallel without the addition of EPS. All of the tested wells contained a final volume of 200 μ L per well. All of the cultures were grown at 37 °C and 150 rpm for 18 hours. Finally, bacterial growth inhibition was quantified by reading the OD of the treatments at 600 nm. The values are given as the mean of 6 biological replicates and their respective standard deviations are reported.

Statistical analysis of Antimicrobial and Antibiofilm Analysis. Statistical analysis was performed using GraphPad Prism version 7.0 (GraphPad Software, San Diego, CA, USA). One way Analysis of Variance (ANOVA), followed by Dunnett's or Tukey's post hoc tests, when appropriate, were used to determine significant differences (P-value < 0.05) between treatments in the antimicrobial and antibiofilm assays. All experiments were performed in biological triplicates and the mean is reported with the corresponding standard deviations.

Fluorescence Microscopy of Microbial Cells. 10⁵ bacterial cells were treated with 0, and 2500 ppm of EPS for 20 hours at 37 °C and 150 rpm. After treatment, cells were stained with 5 μ g/mL of Propidium Iodide (PI) for 1 hour at 37 °C-150 rpm. Then, 20 μ L of the control and treated stained cells were spread in a glass slide, previously cleaned with 96% ethanol. The sample was allowed to air dry and the slides were then fixed by adding 200 μ L of absolute methanol for 2 minutes. Methanol excess was decanted and slides were washed twice with PBS. Images were acquired with a LEICADM 3000 using the 100X objective with a Filter system Y3 ET.

Citotoxicity of Exopolysaccharide. *Cell culture.* H9c2 cells (ATCC, Manassas, VA, USA) were plated in 12-well trays at a concentration of 2 \times 10⁴ cells per well in DMEM media supplemented with 10% fetal bovine serum (FSB), penicillin (100 U/mL) and streptomycin (100 μ g/mL). After reaching 70–80% confluence the cells were treated with different concentrations 5,000 ppm, 2500 ppm, 2000 ppm, 1000 ppm, 500 ppm, 250 ppm, 125 ppm and 75 ppm of EPS for 24 h at 37 °C in an atmosphere composed of 95% air and 5% CO₂. A culture with no EPS added was grown in parallel as a control.

Assessment of apoptosis and necrosis by flow cytometry. H9c2 cells plated in 12-well trays at a concentration of 2 \times 10⁴ cells per well in 1 mL DMEM media, were treated with 5,000 ppm, 2500 ppm, 2000 ppm, 1000 ppm, 500 ppm, 250 ppm, 125 ppm and 75 ppm of EPS. After 24hr of incubation the cells were trypsinized and harvested. Approximately 8 \times 10⁴ cells/well were washed with media supplemented with FBS to neutralize the trypsin and centrifuged at 1,400 rpm for 7 min, at room temperature. After washing the cells 2 times in media, the cells were resuspended in a Tyrode solution in Falcon FACS tubes (Corning, Life Sciences, Mexico).

To assess apoptosis, an Annexin V Apoptosis Detection kit conjugated with PE-Cy7 (eBioscience, San Diego, CA, USA) was used. Next, the cells were resuspended in Tyrode solution plus 2.5 mM CaCl₂ and stained with Annexin V. Cells were incubated for 10 minutes at room temperature in the dark. After incubation, a Tyrode plus 2.5 mM CaCl₂ solution was added and the cells were washed at 1,400 RPM for 7 min at room temperature. After

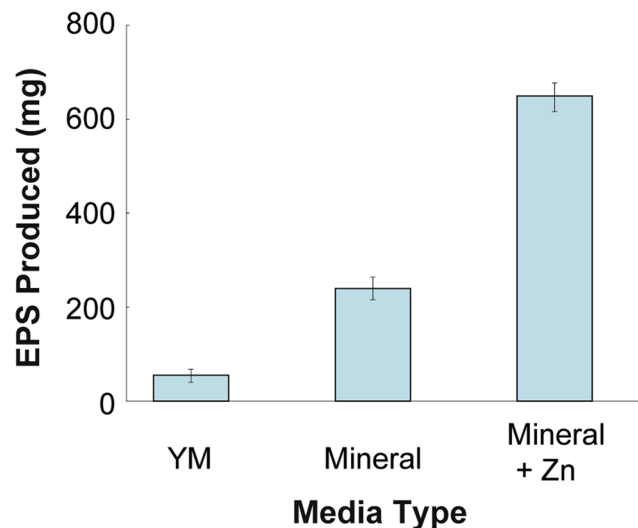


Figure 1. EPS production in different media formulations. EPS production at 72 h, when *R. mucilaginos* UANL-001L is grown in YM media, Mineral Media and Mineral Media + Zn. Mean \pm SD, $n = 3$ error bars are reported.

washing, the cells were resuspended in Tyrode plus 2.5 mM CaCl₂ solution. To assess viability, propidium iodide was added to discard necrotic cells. For each tube 20,000 viable events were recorded. Samples were analyzed with a FACSCanto II (Becton Dickinson, San Jose CA) cytometer with a 488 nm and a 633 nm laser. To analyze the proportions between viable and apoptotic cells, software compensation was performed using Flowjo VX (TreeStar, Oregon, USA). After discarding doublets, Annexin V positive cells were deemed as apoptotic, propidium iodide positive cells were deemed as necrotic, while cells without any staining were deemed as viable cells. As positive controls for apoptosis Staurosporin was used at a concentration of 20 μ M. For necrosis Doxorubicin was used as a control at 30 μ M.

All experiments were performed in biological triplicates and the statistical data are presented as mean \pm standard deviation. Fluorescence values represent the mean of the Median Fluorescence Intensity of each individual assessment. Comparison between samples were performed by Mann Whitney U test or Kruskal-Wallis for three or more samples, followed by Dunnett's, Tukey's or Bonferroni's *post hoc* tests, when appropriate, to compare experimental groups. Differences were considered significant when $p < 0.05$. Data processing, graphs and statistical analysis were performed with GraphPad Prism (V.5.01; La Jolla, CA, USA) and OriginPro 8.1 SR3 v8.1 (OriginLab Corporation, Northampton MA, USA).

In Vivo Murine Toxicity Experiments. All the experiments were performed in accordance to the animal care guidelines of the Guide for the Care and Use of Laboratory Animals published by the US National Institutes of Health (NIH Publication No. 85-23, revised 1996). The animal use and care committee of the Tecnológico de Monterrey-Medical School approved all procedures. Female C57BL/6 mice (6–8 weeks of age) received a single dose of EPS (2000 mg/Kg of body weight) by gavage³⁰. The maximum dose was chosen based on the OECD 423 protocol³¹. The animals were weighed daily during a week. Mice were examined for behavioral changes or any clinical sign of toxicity every hour during the first 8 h following the treatment and thereafter once a day for a week. Later, the mice were euthanized with a lethal dose of sodium thiopental administered intraperitoneally. After euthanasia, all animals were submitted to necropsy and organs were macroscopically inspected for any abnormality. Hematocrit, leucocytes and erythrocytes were measured and compared with untreated mice.

Results and Discussion

Kinetics of Cellular Growth and EPS production. Three different growth media were explored in order to determine the optimal components that stimulated EPS biosynthesis in *R. mucilaginos* UANL-001L. Our research group previously found that *R. mucilaginos* UANL-001L increases EPS biosynthesis in the presence of different heavy metals²⁵. Therefore, the difference in composition between the YM media and the other two media tested was the addition of Zn and other transition metals (K, Na, Mg and Ca). As can be observed from Fig. 1, EPS biosynthesis is increased when transition metals are added to the media. When compared with EPS produced by *R. mucilaginos* grown in YM alone, EPS biosynthesis is increased by 900%, when *R. mucilaginos* is grown in YM media with added K, Na, Mg and Ca, and 3000% when it is grown in YM media with added K, Na, Mg, Ca and Zn.

EPS biosynthesis in *R. mucilaginos* UANL-001L was further studied in the best performing medium (YM-Mineral-Zn) as a function of cellular growth. Under experimental conditions, stationary phase was reached at 48 hours with an estimate of 8.2×10^7 CFU/mL (Fig. 2A). Exopolysaccharide biosynthesis began at exponential phase at 12 hours, reaching the highest EPS production yield (19 mg/mL) at 96 hours (Fig. 2B). These results correlate with the data obtained recently by our research group²⁵.

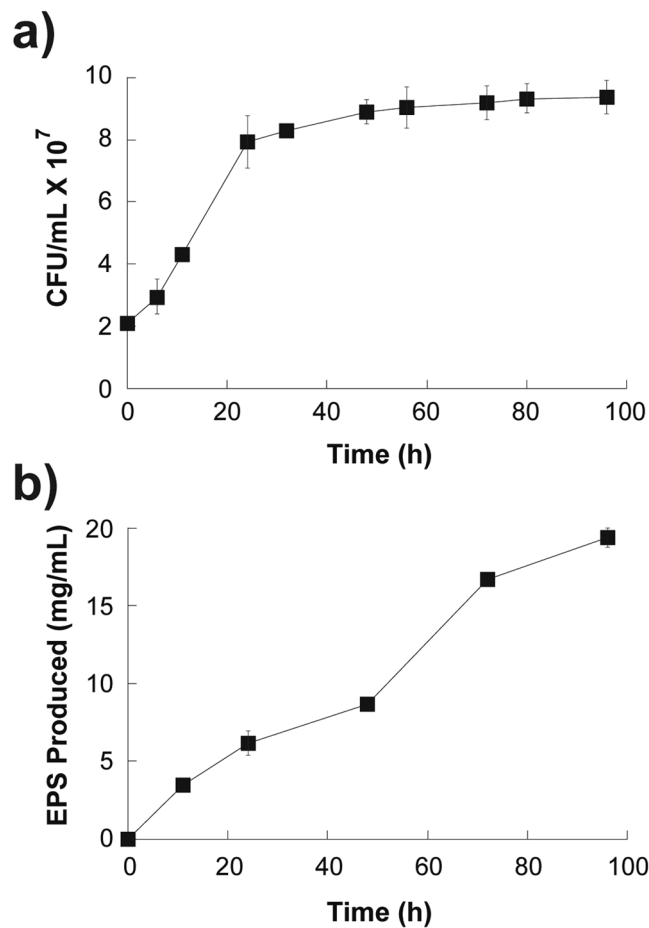


Figure 2. EPS biosynthesis as a function of cellular growth. (A) Cell growth kinetics for 96 h. (B) EPS production kinetics for 96 h. Mean \pm SD, $n = 3$ error bars are reported.

The results show that the exopolysaccharide is mainly produced when the microbial culture is in the stationary phase. It might be assumed that when the stationary phase is reached, the metabolic pathway changes to EPS production, instead of cellular growth, as has been described by other authors^{32,33}.

EPS Production in a *Rhodotorula mucilaginosa* UANL-001L – *E. coli* coculture. In order to explore EPS production by *R. mucilaginosa* UANL-001L in the presence of another microorganism; a set of experiments were performed where the *R. mucilaginosa* initial inoculum concentration was maintained constant and glucose and the initial inoculum of *E. coli* were varied between 3 levels (low, medium and high). As can be observed from Fig. 3, in general, EPS production in the cocultures is increased between 10 and 80%, when compared to EPS production when *R. mucilaginosa* UANL-001L is grown alone. Moreover, for each of the initial *E. coli* inoculum experiments, doubling glucose concentrations from 5 to 10 g/L is not sufficient to increase EPS production (Fig. 3). This is a common phenomenon since it has been previously reported that metabolite biosynthesis does not correlate linearly with the amount of carbon sources in the media^{34,35}. It can be suggested that at these coculture conditions the carbon source is still limited and therefore the EPS production is not increased. However, when glucose concentration is raised to 15 g/L, the carbon source is less limiting, especially for the 3×10^6 *E. coli* initial inoculum, and the *E. coli* initial concentration plays a different effect, triggering a 2.5 fold increase in EPS production. For the low 1×10^6 initial inoculum concentration, even though EPS production is increased by almost 40% compared to EPS production in *R. mucilaginosa* grown alone, the results also show that production is kept almost constant, independent of increases in the amount of glucose added (Fig. 3). Together, these results show that, like in other coculture systems reported in the literature, EPS production depends on the interaction between carbon source availability and the initial size of the *E. coli* inoculum³⁶. These results also suggest that EPS production in *R. mucilaginosa* UANL-001L is a mechanism of defense triggered by the presence of a competing bacterial species; a phenomenon that has been observed in both bacterial and fungi species.

Chemical Characterization of the EPS using FT-IR. Chemical characterization of the biosynthesized exopolysaccharide was first performed through FT-IR. The spectrum is shown in Fig. 4a where different regions of interest are observed. The peak at $3600\text{--}3200\text{ cm}^{-1}$ was assigned to hydroxyl groups from polysaccharide³⁷. The weak peak at approximately 2920 cm^{-1} corresponds to CH_2 , a band at $1650\text{--}1540\text{ cm}^{-1}$ corresponds usually to enol and amide groups¹⁹. The absorption peak at approximately 1365 cm^{-1} corresponds to carboxyl groups³⁸.

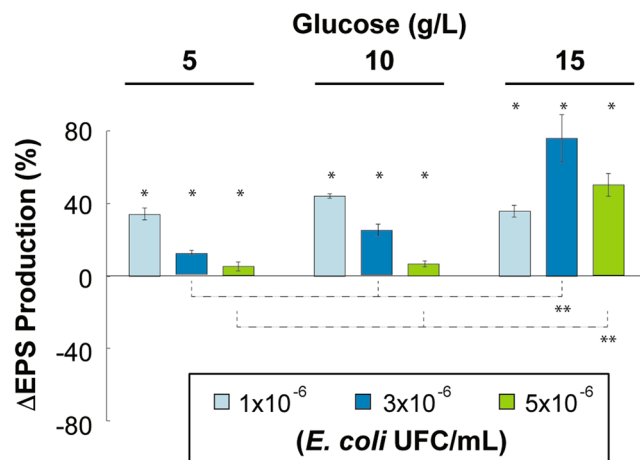


Figure 3. EPS biosynthesis in *R. mucilaginosa* UANL-001L when co-cultured at low, medium and high levels of *E. coli* initial inoculum and glucose concentration in the media. EPS production after 72 h of co-culture is reported as a percentage increase compared to EPS production when *R. mucilaginosa* UANL-001L is grown alone. Mean \pm SD, $n = 3$ error bars are reported. A (*) above the bar represents a $P < 0.05$ between groups at same glucose concentration. A (**) above the bars represent a $P < 0.05$ between groups at same initial *E. coli* inoculum.

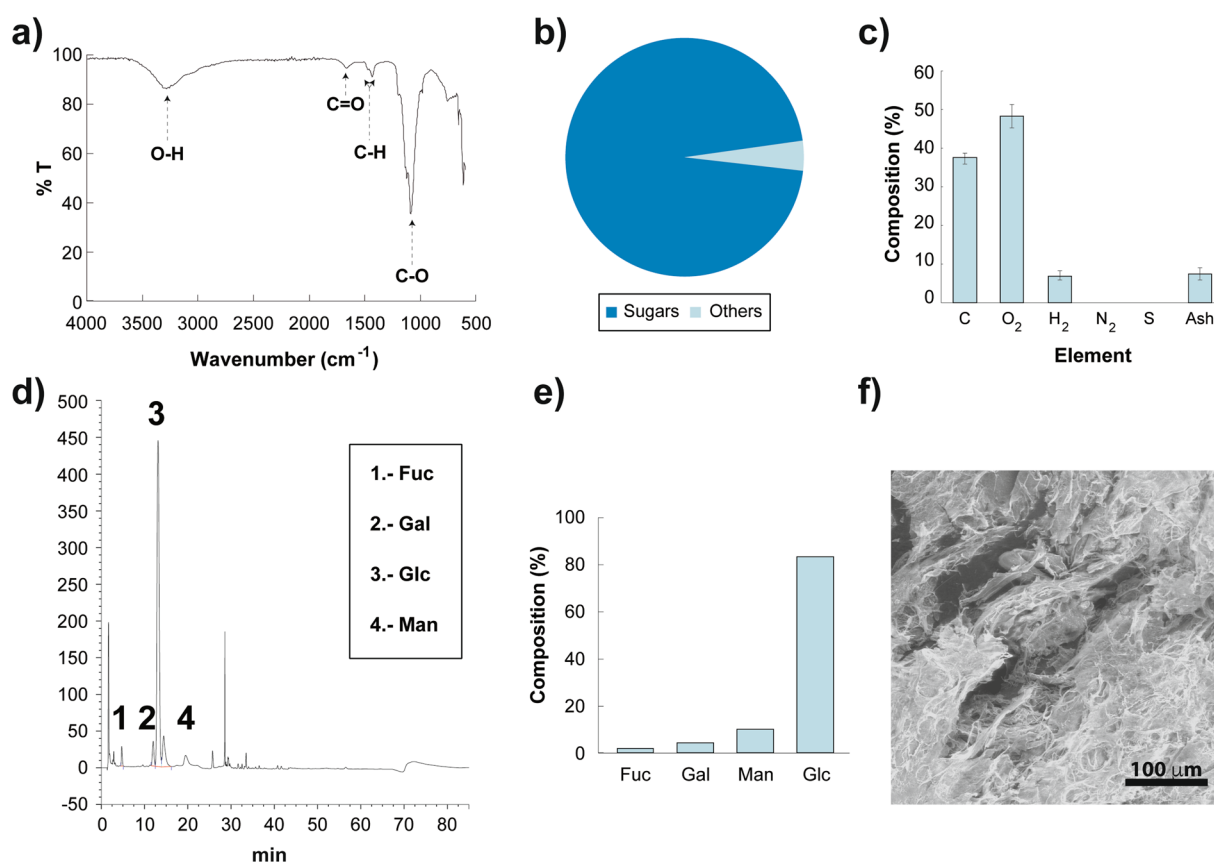


Figure 4. Chemical and Physical Properties of the EPS biosynthesized by *R. mucilaginosa* UANL-001L. The data show chemical and physical analysis of the EPS produced by *Rhodotorula mucilaginosa* UANL-001L. (a) FTIR of the EPS with the different peaks highlighted and tagged with the chemical group corresponding to each specific wavenumber. (b) Percentage of carbohydrates present in the EPS. (c) C, O, H, N, S and ashes percentage composition of the exopolysaccharides. (d) GC-MS spectrum of EPS produced by *R. mucilaginosa* UANL-001L, with all of the monosugars detected labeled. (e) Composition of each of the monosugars present in the EPS. (f) SEM image showing morphology of EPS.

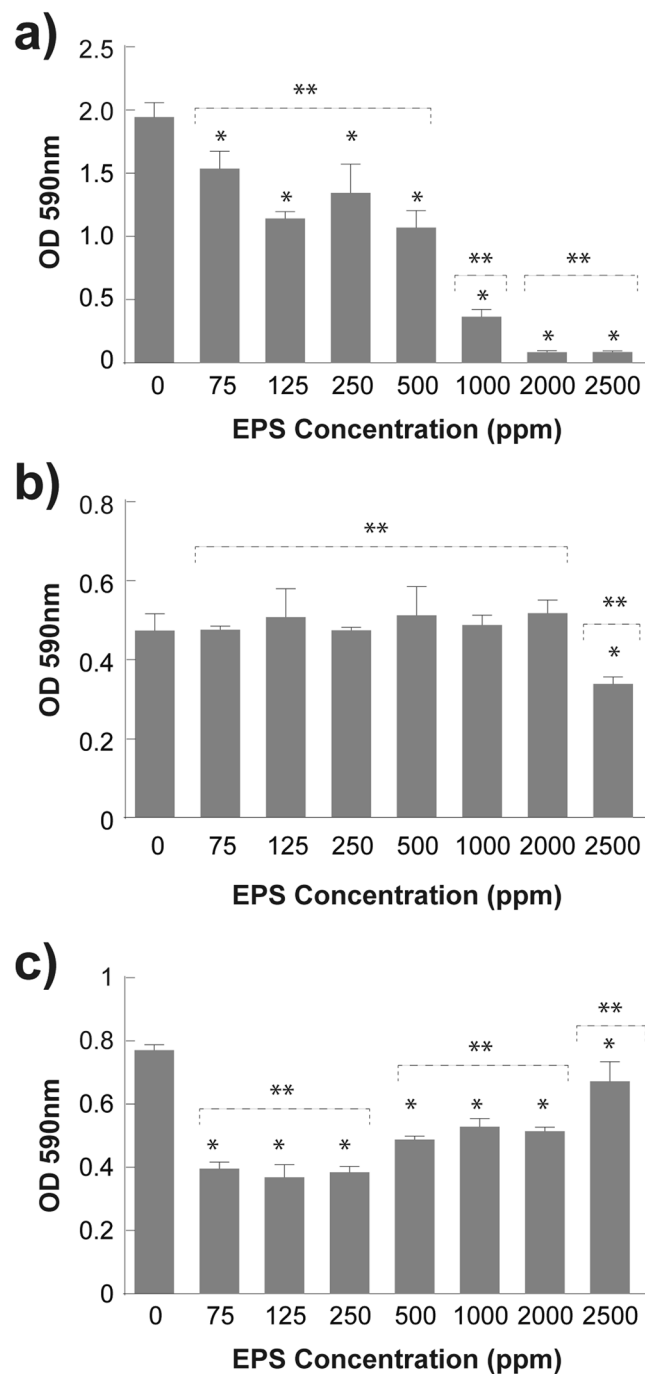


Figure 5. Antibiofilm Activity of the EPS biosynthesized by *R. mucilaginosa* UANL-001L. Biofilm formation is measured after the treatment of bacterial cultures with a range of EPS concentrations. The results correspond to (a) *S. aureus* ATCC 6538, (b) *P. aeruginosa* ATCC 27853 and (c) *E. coli* ATCC 11229. Mean \pm SD, n = 3 error bars are reported. A (*) above the bar represents a $P < 0.05$ between treatments and the control. A (**) above the bars represent a $P < 0.05$ between groups of treatments.

Finally, the broad stretch region from $1000\text{--}1200\text{ cm}^{-1}$ corresponds to the C-O, C-C stretching, C-O-C and C-O-H deformation vibrations of polysaccharides. The strongest peak at 1084 cm^{-1} was an indicative that the sample is a polysaccharide³⁹.

Furthermore, to decipher the chemical groups contributing to the 1649 cm^{-1} wavelength, a chemical assay using 2,4-dinitrophenylhydrazine was performed to detect the presence of carbonyl (C=O) groups in the samples. The assay resulted positive for the presence of carbonyl groups in the EPS. Next, through an initial qualitative elemental analysis, amino and amido groups were discarded due to the absence of nitrogen in the samples. Together, these chemical assays show that the absorption band at 1649 cm^{-1} corresponds to the C=O stretching vibration in the carbonyl groups.

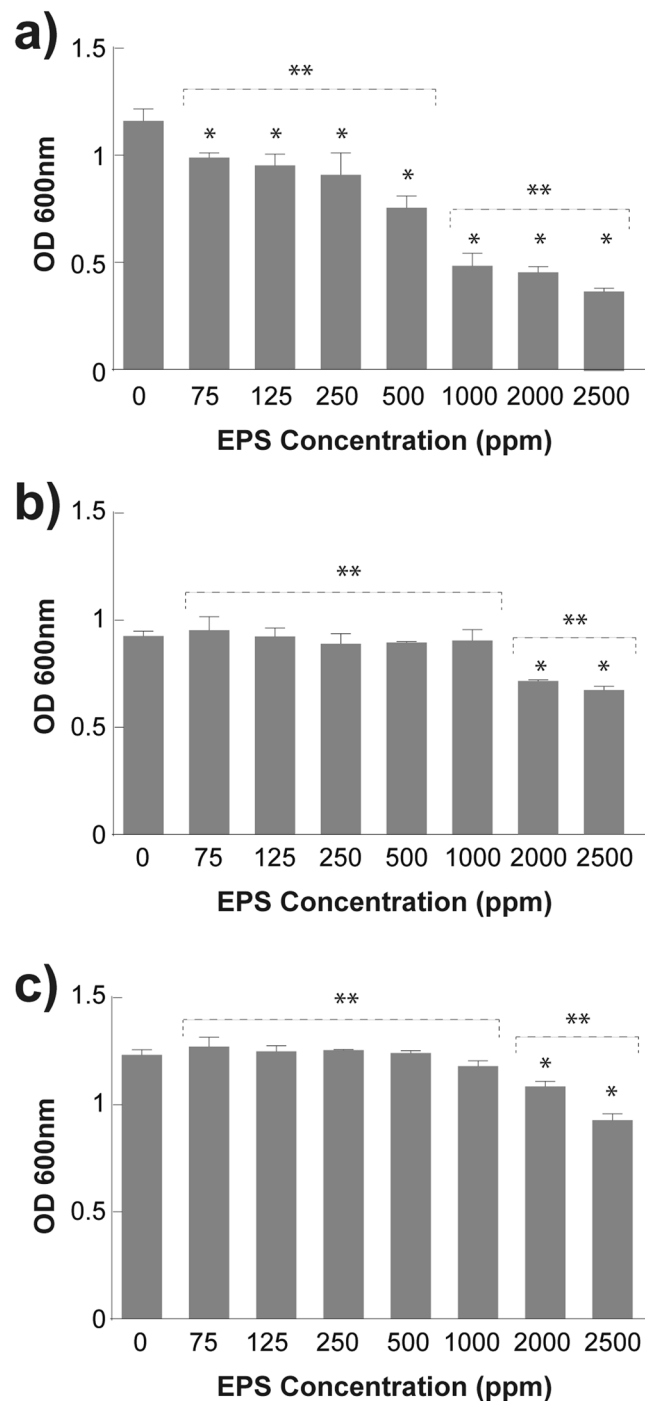


Figure 6. Antimicrobial Activity of the EPS biosynthesized by *R. mucilaginosa* UANL-001L. Microbial growth in liquid culture is measured after the treatment of bacterial cultures with a range of EPS concentrations. The results correspond to (a) *S. aureus* ATCC 6538, (b) *P. aeruginosa* ATCC 27853 and (c) *E. coli* ATCC 11229. Mean \pm SD, n = 3 error bars are reported. A (*) above the bar represents a $P < 0.05$ between treatments and the control. A (**) above the bars represent a $P < 0.05$ between groups of treatments.

Total amount of carbohydrates in the EPS was quantified through the Debois method. The total percentage of carbohydrates in the samples ranged from 91 to 96% with variations of only 5% (Fig. 4b). Furthermore, quantitative data was obtained using an Elemental Analyzer. As shown in Fig. 4c, carbon, hydrogen and oxygen made up for 93% of the total samples. The results again demonstrate the absence of N and S in the samples; confirming that amino and amido groups were absent in the EPS produced (Fig. 4c).

Monosaccharide composition analysis. The EPS samples were further characterized through an HPAEC-PAD analysis. Figure 4d, shows that the EPS are composed of the following monosaccharides: fucose,

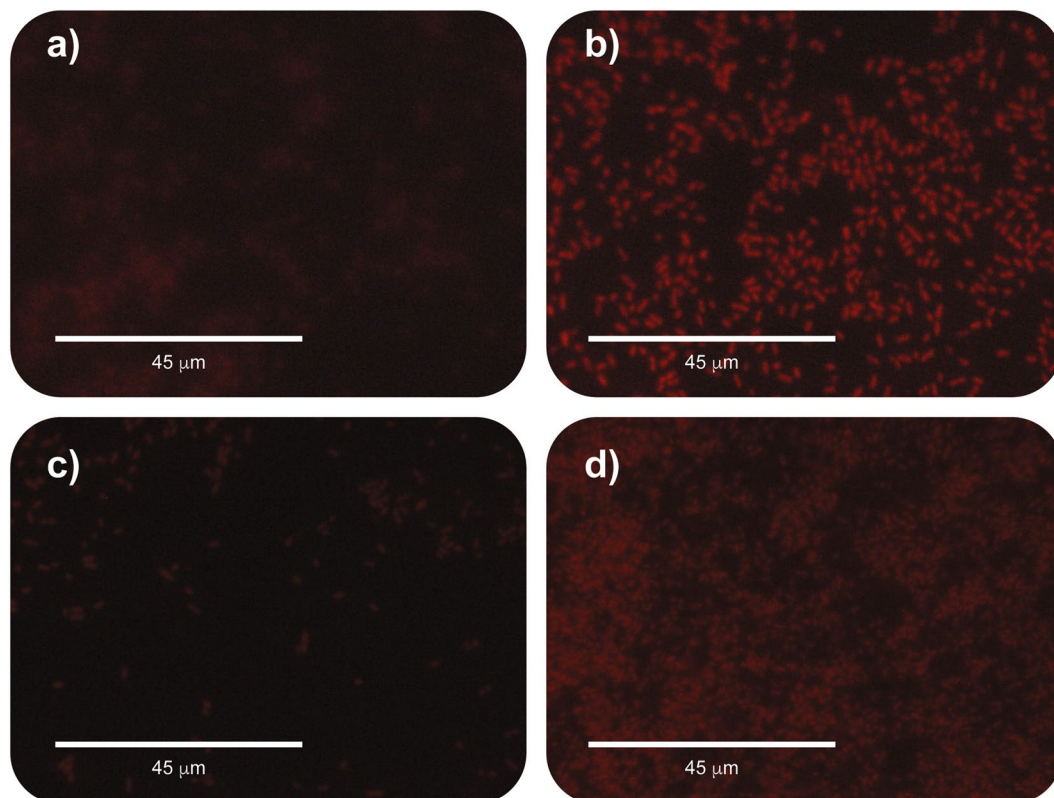


Figure 7. Permeability assay of *E. coli* and *P. aeruginosa* treated with EPS. Fluorescence micrographs of PI stained bacteria. (a) Control untreated *E. coli*; (b) *E. coli* treated with 2500 ppm of EPS; (c) Control untreated *P. aeruginosa*; (d) *P. aeruginosa* treated with 2500 ppm of EPS.

galactose, mannose and glucose. The most abundant monosaccharide in the composition of the EPS is glucose with 82%, followed by mannose, galactose and fucose, with the least contribution to the composition (Fig. 4e). After hydrolysis there were no uronic acids in the sample, suggesting that the multiple peaks of glucose shown in the GC-MS spectrum, correspond to intact ring forms of sugars present in different configurations⁴⁰. Subsequently, the presence of these sugars was confirmed by matching the retention time of known monosaccharide standards with the GC-MS spectrum. The composition of the exopolysaccharide reported in this work indicates that it is a novel biopolymer produced by the *R. mucilaginosa* UANL-001L strain. The exopolysaccharide here reported resembles the composition of other microbial EPS that have glucose as their main monosaccharide⁴¹. Moreover, its composition is very similar to a mannose-rich acidic heteropolysaccharide, produced by *R. glutinis* KCTC 7989, and composed of 85% of neutral sugars (fucose, mannose, galactose, and glucose) and 15% uronic acid^{33,42}.

Physical Properties of EPS using SEM. Through size exclusion chromatography, the molecular weight of the EPS was found to be 18.85 kDa, considered a low molecular weight biopolymer compared to EPS produced by other microorganisms⁴³. The EPS morphology was analyzed using an SEM since it is a technique that can be used to provide insights of physical properties⁴⁴. The micrographs of the EPS from *R. mucilaginosa* UANL-001L show that the EPS exhibit a compact and granular surface (Fig. 4f), suggesting that these polysaccharides might have gelling and emulsifying properties^{39,44}. Due to the aforementioned characteristics, this polysaccharide could be applied as a thickener, stabilizer and as an emulsifier agent in the food and cosmetic industry. Moreover, this polymer could be used to develop encapsulation technologies for the delivery of drugs or bioactive compounds⁴⁵.

Antibiofilm activity. Antibiofilm activity of EPS was analyzed against one Gram positive (*S. aureus* ATCC 6538) and two Gram negative (*E. coli* ATCC 11229 and *P. aeruginosa* ATCC 27853) strains, in order to determine the antimicrobial spectrum of the exopolysaccharide.

The effect of EPS on biofilm formation is reported in Fig. 5. EPS presents a dose-dependent inhibitory effect on *S. aureus* biofilm formation, inhibiting 81% of biofilm formation when a concentration of 1000 ppm was used (Fig. 5a). When higher concentrations of EPS (2000 ppm and 2500 ppm) were used, further inhibition (96%) was shown (Fig. 5a). EPS from *Rhodotorula mucilaginosa* UANL-001L exhibits a higher antibiofilm activity at minor concentrations compared to EPS from *Lactobacillus plantarum* YW32 (5 mg/mL) and *Streptococcus phocae* PI80 (5 mg/mL), which inhibited biofilm formation by 45% and 51%, respectively^{17,46}.

The addition of *R. mucilaginosa* EPS at 2500 ppm was able to inhibit 30% of *P. aeruginosa* biofilm formation (Fig. 5b). Similar to the *R. mucilaginosa* EPS activity, r-EPS (1 mg/mL) from *Lactobacillus acidophilus* A4,

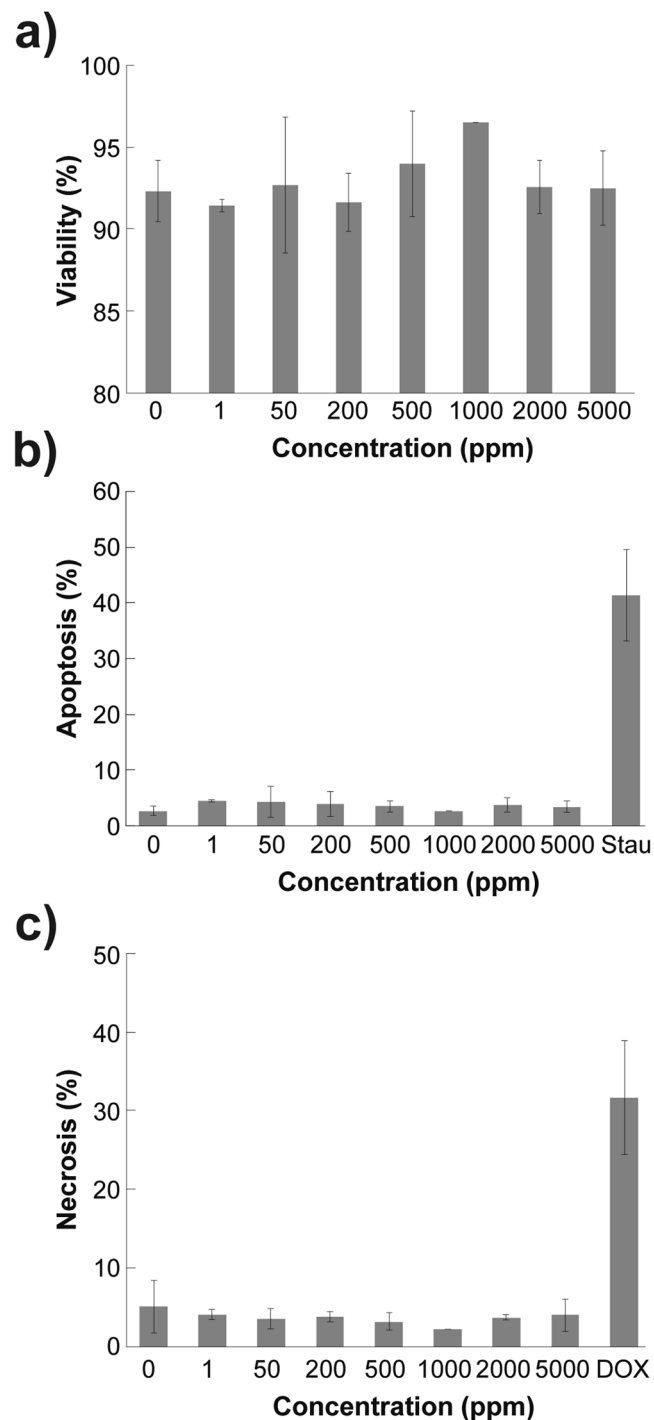


Figure 8. A dose range of 0.1–5000 $\mu\text{g}/\text{mL}$ EPS does not induce apoptosis or necrosis after 24 hrs. There were no differences in the percentage of induction of necrosis or apoptotic in a dose dependent setting. **(a)** Viable cells, **(b)** Apoptotic cells and **(c)** Necrotic cells. Results are means \pm S.D. $n = 3-6$, p values for viability $p = 0.83$, apoptosis $p = 0.6$ and necrosis $p = 0.8$.

which was able to reduce biofilm formation by 40%⁴⁷. Such is also the case of EPS (1 mg/mL) from *E. faecium* MC13, capable of reducing *P. aeruginosa* biofilm by 15%⁴⁸. Moreover, a reduction of 86% on biofilm formation was achieved by a treatment with B4-EPS1 from *Arthrobacter sp. B4* at a lower concentration (50 $\mu\text{g}/\text{mL}$)⁴⁹. For the case of biofilm formed by *E. coli* (Fig. 5c), the results show that biofilm formation was reduced when lower concentrations of *R. mucilaginosa* EPS (250 ppm, 125 ppm and 75 ppm) were added. In contrast, biofilm formation was recovered at higher concentrations (2500 ppm, 2000 ppm, 1000 ppm, 500 ppm). Similar results have been reported before, the capsular polysaccharide of *Vibrio sp. QY101* stimulated biofilm establishment of

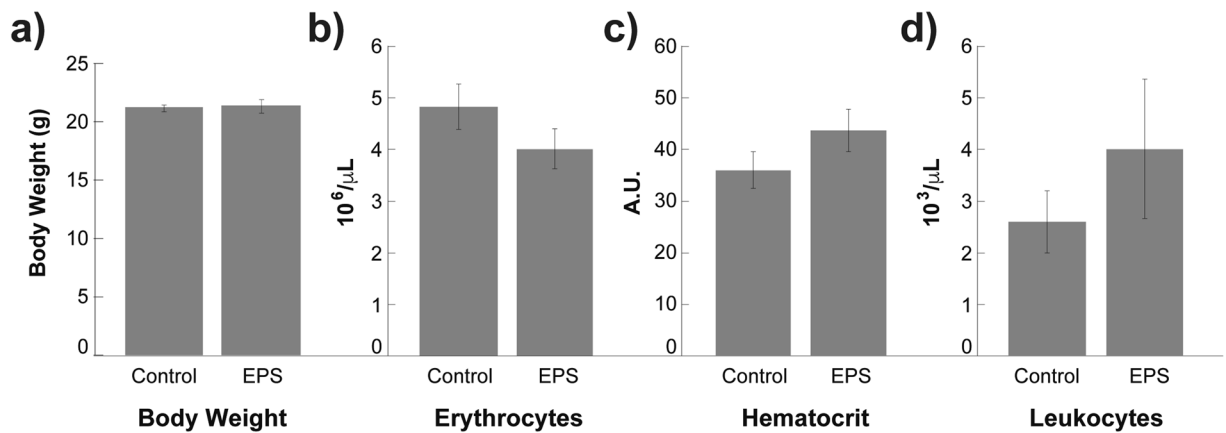


Figure 9. Murine Model Shows No Cytotoxicity of EPS. There were no statistical differences between control and the treated mice in: (a) Body Weight ($p = 0.82$); (b) Erythrocytes ($p = 0.21$); (c) Hematocrit ($p = 0.23$); (d) Leukocytes ($p = 0.39$). Results are means \pm S.D, $n = 3$.

P. aeruginosa ATCC27853, *S. aureus* and *E. faecalis* OG1RF⁵⁰. Therefore, *Rhodotorula* EPS may induce an unidentified mechanism in *E. coli* cells that enables biofilm formation at higher EPS concentrations.

EPS from *R. mucilaginosa* exhibited antibiofilm activity against Gram-positive and Gram-negative bacteria. In fact, some authors had reported that exopolysaccharides are able to interfere with cell-surface interaction (initial adhesion of biofilm development) via modification of physicochemical properties of biotic and abiotic surfaces, inhibition of cell to cell interaction and downregulation of biofilm-forming genes²⁴.

These EPS antibiofilm properties unblock potential applications in health and industrial settings, where bacterial cells form biofilms to colonize tissues and medical devices or attach to surfaces affecting industrial process. The EPS produced by *R. mucilaginosa* UANL-001L has very interesting applications as an antiadhesive or antibiofouling agent to prevent bacterial biofilm formation.

Bacterial Growth inhibition. EPS antibacterial activity was measured in order to explore its toxicity against both bacterial models. Different EPS concentrations were used against *E. coli*, *S. aureus* and *P. aeruginosa*, displaying diverse effects amongst the tested bacteria. (Fig. 6).

A dose-dependent inhibitory effect was observed when serial concentrations of EPS were used against *S. aureus* (Fig. 6a). EPS at concentrations between 1000 and 2500 ppm, showed the strongest antibacterial activity, inhibiting 60% of bacterial growth (Fig. 6a). Similarly, *E. coli* (Fig. 6b) and *P. aeruginosa* (Fig. 6c) were susceptible to EPS at 2000 and 2500 ppm, inhibiting bacterial growth at 27% and 24%, respectively. Although the exact antibacterial mechanism of the EPS from *Rhodotorula mucilaginosa* UANL-001L remains unclear some authors have suggested that microbial exopolysaccharides could modify and disrupt bacterial cell surface leading to the leakage of intracellular proteins and metabolites, which results in cell death^{16,51}. Moreover, based on the literature published, this is the first report on antibiofilm and bactericidal activity exhibited by EPS produced in *R. mucilaginosa*.

Insight into the Antimicrobial Mechanism of Action. An insight into the antimicrobial mechanism of action was sought through the analysis of bacterial membrane disruption, using a fluorescence PI stain⁵², after EPS treatments. As observed in the micrographs, *E. coli* (Fig. 7b) and *P. aeruginosa* (Fig. 7d) treated with 2500 ppm of EPS show, qualitatively, increased fluorescence compared to the untreated *E. coli* (Fig. 7a) and *P. aeruginosa* (Fig. 7c). These results, combined with the data on antimicrobial activity, show that even when the exopolysaccharide has a low growth inhibition on the bacterial strains (2500 ppm), the EPS obtained from *R. mucilaginosa* disrupts membrane integrity and causes an increase in cell permeability. This can be hypothesized to be at least one of the EPS's mechanisms of antimicrobial action against competing microorganisms. Moreover, this surface interaction between the *R. mucilaginosa* EPS and the membrane of the bacteria, could be one of the antibiofilm mechanisms since the disruptive interaction would act as an anti-adhesive²³. Antibiofilm exopolysaccharides have been reported to modify the physical properties of biotic and abiotic surfaces²⁴. Thus, the antibacterial and antibiofilm effect of the EPS reported in this work may be caused by modification of the *E. coli* and *P. aeruginosa* cell membrane.

Exopolysaccharide Cytotoxicity. In order to assess the cytotoxic effects of EPS in a biological/translational setting we tested different concentrations *in-vitro* with a relevant cell line. H9c2 cells are cardiac ventricular myoblasts that resemble the functionality of cardiac myocytes. The results in Fig. 8a show that EPS was not toxic, since viability remained constant above 92%, using doses ranging between 0–5000 $\mu\text{g}/\text{mL}$. There were no statistical differences between each of the doses ($p = 0.83$). The frequencies of both mean apoptotic (Fig. 8b) and necrotic cells (Fig. 8c) were maintained at values below 5%, with no statistical difference between them ($p = 0.6$ and $p = 0.8$, respectively). Moreover, we tested positive controls for apoptosis and necrosis. Cells were treated with Staurosporin, as a positive control for apoptosis, and with Doxorubicin, as a positive control for necrosis. The

results show a 40% of apoptosis for the Staurosporin treatment and a 32% of necrotic cells for the Doxorubicin treatment. Together, these results demonstrate that the EPS does not exhibit cytotoxic effects to the tested cell line.

Exopolysaccharide Cytotoxicity *In Vivo*. A murine cytotoxicity model was performed to test effects of EPS from *R. mucilaginosa* UANL-001L. No deaths or any other clinical or behavioral signs of toxicity were observed in mice treated with EPS. All EPS-treated mice (2000mg/kg bw po) maintained their body weight throughout 1 week post-treatment. The mean body weight between the untreated and EPS treated mice showed no statistically significant differences (Fig. 9a). Blood tests results show that there were no differences in erythrocyte (Fig. 9b), hematocrit (Fig. 9c) and leukocyte (Fig. 9d) counts between the treated and untreated mice. In addition, no gross pathological abnormality was observed in major organs at necropsy, therefore histology was considered unnecessary. Since this EPS upper limit dose caused no deaths or any other discernible signs of toxicity, lower doses were not tested

Conclusions

The novel strain *Rhodotorula mucilaginosa* UANL 001 L produces a non-cytotoxic novel exopolysaccharide that presents interesting antibiofilm and antimicrobial properties. This is the first report of an antimicrobial and antibiofilm EPS produced by yeast of the genera *Rhodotorula*. All the bacterial strains tested in this study were susceptible to the inhibitory activity of the EPS, particularly; the bacterial growth and biofilm formation of *Staphylococcus aureus* were inhibited in a higher degree. Since *S. aureus* is one of the most important pathogens in human health, the EPS could be formulated as an antiadhesive and antibiofilm treatment for medical and non-medical applications.

References

- Walsh, C. & Wright, G. (ACS Publications, 2005).
- Morones-Ramirez, J. R. Plata metal precioso con amplio espectro de aplicaciones. *Revista Ciencia y Desarrollo* **36**, 56–62 (2010).
- Morones-Ramirez, J. R., Winkler, J. A., Spina, C. S. & Collins, J. J. Silver enhances antibiotic activity against gram-negative bacteria. *Science translational medicine* **5**, 190ra181–190ra181 (2013).
- Morones-Ramirez, J. R. & Gallegos-López, S. Plata, Metal con Brillante Futuro en la Medicina. *Ciencia y Desarrollo* **2014**, 8 (2014).
- Tan, Y.-T., Tillett, D. J. & McKay, I. A. Molecular strategies for overcoming antibiotic resistance in bacteria. *Molecular medicine today* **6**, 309–314 (2000).
- Patel, R. Biofilms and antimicrobial resistance. *Clinical orthopaedics and related research* **437**, 41–47 (2005).
- Coenye, T. & Nelis, H. J. *In vitro* and *in vivo* model systems to study microbial biofilm formation. *Journal of microbiological methods* **83**, 89–105 (2010).
- Bryers, J. D. Medical biofilms. *Biotechnology and bioengineering* **100**, 1–18 (2008).
- Penesyan, A., Gillings, M. & Paulsen, I. T. Antibiotic discovery: combatting bacterial resistance in cells and in biofilm communities. *Molecules* **20**, 5286–5298 (2015).
- Morones, J. R. *et al.* The bactericidal effect of silver nanoparticles. *Nanotechnology* **16**, 2346–2353 (2005).
- Bertrand, S. *et al.* Metabolite induction via microorganism co-culture: a potential way to enhance chemical diversity for drug discovery. *Biotechnology advances* **32**, 1180–1204 (2014).
- Karwehl, S. & Stadler, M. Exploitation of fungal biodiversity for discovery of novel antibiotics. (2016).
- Pavlova, K. I. In *Cold-adapted Yeasts* 397–415 (Springer, 2014).
- Hatoum, R., Labrie, S. & Fliss, I. Antimicrobial and probiotic properties of yeasts: from fundamental to novel applications. *Frontiers in microbiology* **3** (2012).
- Van Bogaert, I. N., De Maeseneire, S. L. & Vandamme, E. J. In *Yeast biotechnology: Diversity and applications* 651–671 (Springer, 2009).
- He, F., Yang, Y., Yang, G. & Yu, L. Studies on antibacterial activity and antibacterial mechanism of a novel polysaccharide from *Streptomyces virginia* H03. *Food Control* **21**, 1257–1262 (2010).
- Wang, J., Zhao, X., Yang, Y., Zhao, A. & Yang, Z. Characterization and bioactivities of an exopolysaccharide produced by *Lactobacillus plantarum* YW32. *International journal of biological macromolecules* **74**, 119–126 (2015).
- Li, S. & Shah, N. P. Antioxidant and antibacterial activities of sulphated polysaccharides from *Pleurotus eryngii* and *Streptococcus thermophilus* ASCC 1275. *Food chemistry* **165**, 262–270 (2014).
- Zhang, J. *et al.* Physicochemical characteristics and bioactivities of the exopolysaccharide and its sulphated polymer from *Streptococcus thermophilus* GST-6. *Carbohydrate polymers* **146**, 368–375 (2016).
- Mahapatra, S. & Banerjee, D. Fungal exopolysaccharide: production, composition and applications. *Microbiology insights* **6**, 1 (2013).
- Jittawuttipoka, T. *et al.* Multidisciplinary evidences that *Synechocystis* PCC6803 exopolysaccharides operate in cell sedimentation and protection against salt and metal stresses. *PLoS one* **8**, e55564 (2013).
- Nadell, C. D., Drescher, K., Wingreen, N. S. & Bassler, B. L. Extracellular matrix structure governs invasion resistance in bacterial biofilms. *The ISME journal* **9**, 1700–1709 (2015).
- Bernal, P. & Llamas, M. A. Promising biotechnological applications of antibiofilm exopolysaccharides. *Microbial biotechnology* **5**, 670–673 (2012).
- Rendueles, O., Kaplan, J. B. & Ghigo, J. M. Antibiofilm polysaccharides. *Environmental microbiology* **15**, 334–346 (2013).
- Garza, M. T. G. *et al.* Metal-Induced Production of a Novel Bioadsorbent Exopolysaccharide in a Native *Rhodotorula mucilaginosa* from the Mexican Northeastern Region. *PLoS one* **11**, e0148430 (2016).
- DuBois, M., Gilles, K. A., Hamilton, J. K., Rebers, P. & Smith, F. Colorimetric method for determination of sugars and related substances. *Analytical chemistry* **28**, 350–356 (1956).
- Praveen, P. S., Anupama, B., Jagathi, V. & Rao, G. D. Spectrophotometric determination of Tolperisone using 2, 4-dinitrophenylhydrazine reagent. *Int J Res Pharm Sci* **3**, 317–320 (2010).
- Tucker, S. H. A lost centenary: Lassaigne's test for nitrogen. *The identification of nitrogen, sulfur, and halogens in organic compounds. J. Chem. Educ* **22**, 212 (1945).
- O'Toole, G. A. Microtiter dish biofilm formation assay. *JoVE (Journal of Visualized Experiments)*, e2437–e2437 (2011).
- Castorena-Torres, F. *et al.* Natural Foliates from Biofortified Tomato and Synthetic 5-methyl-tetrahydrofolate Display Equivalent Bioavailability in a Murine Model. *Plant Foods for Human Nutrition* **69**, 57–64, <https://doi.org/10.1007/s11130-013-0402-9> (2014).
- Pinto, F. C. M. *et al.* Acute toxicity, cytotoxicity, genotoxicity and antigenotoxic effects of a cellulosic exopolysaccharide obtained from sugarcane molasses. *Carbohydrate Polymers* **137**, 556–560, 10.16/j.carbpol.2015.10.071 (2016).
- Kim, J. H., Kim, E. Y. & Chu, K. H. In *Advanced Materials Research*. 1048–1051 (Trans Tech Publ).

33. Cho, D. H., Chae, H. J. & Kim, E. Y. Synthesis and characterization of a novel extracellular polysaccharide by *Rhodotorula glutinis*. *Applied biochemistry and biotechnology* **95**, 183–193 (2001).
34. Lee, W. Y., Park, Y., Ahn, J. K., Ka, K. H. & Park, S. Y. Factors influencing the production of endopolysaccharide and exopolysaccharide from *Ganoderma applanatum*. *Enzyme and Microbial Technology* **40**, 249–254, <https://doi.org/10.1016/j.enzmictec.2006.04.009> (2007).
35. Cerning, J. *et al.* Carbon Source Requirements for Exopolysaccharide Production by *Lactobacillus casei* CG11 and Partial Structure Analysis of the Polymer. *Applied and Environmental Microbiology* **60**, 3914–3919 (1994).
36. Lin, E.-S. & Chen, Y.-H. Factors affecting mycelial biomass and exopolysaccharide production in submerged cultivation of *Antrrodia cinnamomea* using complex media. *Bioresource Technology* **98**, 2511–2517, <https://doi.org/10.1016/j.biortech.2006.09.008> (2007).
37. Subudhi, S. *et al.* Purification and characterization of exopolysaccharide bioflocculant produced by heavy metal resistant *Achromobacter xylosoxidans*. *Carbohydrate polymers* **137**, 441–451 (2016).
38. Sathiyarayanan, G. *et al.* Synthesis of carbohydrate polymer encrusted gold nanoparticles using bacterial exopolysaccharide: a novel and greener approach. *RSC Advances* **4**, 22817–22827 (2014).
39. Liu, Y., Gu, Q., Ofosu, F. K. & Yu, X. Production, structural characterization and gel forming property of a new exopolysaccharide produced by *Agrobacterium* HX1126 using glycerol or d-mannitol as substrate. *Carbohydrate polymers* **136**, 917–922 (2016).
40. Cui, W., Wood, P. J., Blackwell, B. & Nikiforuk, J. Physicochemical properties and structural characterization by two-dimensional NMR spectroscopy of wheat β -D-glucan—comparison with other cereal β -D-glucans. *Carbohydrate Polymers* **41**, 249–258, [https://doi.org/10.1016/S0144-8617\(99\)00143-5](https://doi.org/10.1016/S0144-8617(99)00143-5) (2000).
41. Moscovici, M. Present and future medical applications of microbial exopolysaccharides. *Frontiers in Microbiology* **6**, 1012, <https://doi.org/10.3389/fmicb.2015.01012> (2015).
42. Ghada, S. *et al.* Production and Biological Evaluation of Exopolysaccharide From Isolated *Rhodotorula glutinins* (2017).
43. Shu, C.-H. & Lung, M.-Y. Effect of pH on the production and molecular weight distribution of exopolysaccharide by *Antrrodia camphorata* in batch cultures. *Process Biochemistry* **39**, 931–937, [https://doi.org/10.1016/S0032-9592\(03\)00220-6](https://doi.org/10.1016/S0032-9592(03)00220-6) (2004).
44. Costa, N. *et al.* Rheological, microscopic and primary chemical characterisation of the exopolysaccharide produced by *Lactococcus lactis* subsp. *cremoris* DPC6532. *Dairy Science & Technology* **92**, 219–235 (2012).
45. Khan, T., Park, J. K. & Kwon, J.-H. Functional biopolymers produced by biochemical technology considering applications in food engineering. *Korean Journal of Chemical Engineering* **24**, 816–826 (2007).
46. Kanmani, P., Yuvaraj, N., Paari, K., Pattukumar, V. & Arul, V. Production and purification of a novel exopolysaccharide from lactic acid bacterium *Streptococcus phocae* PI80 and its functional characteristics activity *in vitro*. *Bioresource Technology* **102**, 4827–4833 (2011).
47. Kim, Y. & Kim, S. H. Released exopolysaccharide (r-EPS) produced from probiotic bacteria reduce biofilm formation of enterohemorrhagic *Escherichia coli* O157: H7. *Biochemical and biophysical research communications* **379**, 324–329 (2009).
48. Kanmani, P. *et al.* Synthesis and functional characterization of antibiofilm exopolysaccharide produced by *Enterococcus faecium* MC13 isolated from the gut of fish. *Applied biochemistry and biotechnology* **169**, 1001–1015 (2013).
49. Li, Y. *et al.* Production, purification, and antibiofilm activity of a novel exopolysaccharide from *Arthrobacter* sp. B4. *Preparative Biochemistry and Biotechnology* **45**, 192–204 (2015).
50. Jiang, P. *et al.* Antibiofilm activity of an exopolysaccharide from marine bacterium *Vibrio* sp. QY101. *PLoS One* **6**, e18514 (2011).
51. Kong, M., Chen, X. G., Xing, K. & Park, H. J. Antimicrobial properties of chitosan and mode of action: a state of the art review. *International journal of food microbiology* **144**, 51–63 (2010).
52. Morones-Ramirez, J. R., Winkler, J. A., Spina, C. S. & Collins, J. J. Silver Enhances Antibiotic Activity Against Gram-Negative Bacteria. *Sci Transl Med* **5** (2013).

Acknowledgements

Paicyt 2016–2017 Science Grant from the Universidad Autónoma de Nuevo León. CONACyT Grants for: Basic science grant 221332, Fronteras de la Ciencia grant 1502 and Infraestructura Grant 279957. All of them for financially supporting this work.

Author Contributions

A.V.R., X.G.V.A., D.B.P., J.A.G.C., and J.R.M.R. designed, performed and analyzed all of the experimental data and wrote the manuscript. E.V.G., H.C.V. and G.G.R. helped in the designed and performed the cytotoxicity experiments and contributed with the discussion and format of the manuscript. J.J.G.L. A.E.G.L. and X.Z. helped in the designed and performed the SEC experiments. M.T.G.G. helped with the format and methodology of the manuscript.

Additional Information

Competing Interests: The authors declare that they have no competing interests.

Publisher's note: Springer Nature remains neutral with regard to jurisdictional claims in published maps and institutional affiliations.



Open Access This article is licensed under a Creative Commons Attribution 4.0 International License, which permits use, sharing, adaptation, distribution and reproduction in any medium or format, as long as you give appropriate credit to the original author(s) and the source, provide a link to the Creative Commons license, and indicate if changes were made. The images or other third party material in this article are included in the article's Creative Commons license, unless indicated otherwise in a credit line to the material. If material is not included in the article's Creative Commons license and your intended use is not permitted by statutory regulation or exceeds the permitted use, you will need to obtain permission directly from the copyright holder. To view a copy of this license, visit <http://creativecommons.org/licenses/by/4.0/>.

© The Author(s) 2018